DESIGN OF A HYSTERETIC NEURAL-TYPE OP-AMP-RC CIRCUIT

G. Kiruthi,* R. C. Ajmera,+ H. Yazdani* and R. Newcomb*

+ Department of Physics
East Carolina University
Greenville, North Carolina 27834

* Electrical Engineering Department
University of Maryland
College Park, Maryland 20742

Abstract

A design formulation is given for an op-amp RC, hysteresis, neural-type pulse circuit. Equations of design are given which allow cascading of first order basic modules for the realization of neural-type pulse microsystems. Experimental verification indicates the practicality of the circuit.

I. Introduction

Neural-type microsystems are electronic systems which realize the pulse handling characteristics of biological neural systems in a form suitable for integrated circuit construction.[1] To date research efforts have been concentrated upon the generation and propagation of action-potential-type pulses in neuristor structures.[2] However, recently some efforts have investigated signal mixing systems.[3-5] In our studies on neural-type microsystems hysteresis was found to occur naturally in such systems.[6] This motivated us to investigate the hysteresis phenomenon[7] and its use in neural-type systems.[8] This has led us to present here a design theory of a neural-type circuit whose operation is based primarily on hysteresis.

Previously we proved the existence of a first order system designed on the basis of binary hysteresis and which exhibits neural type pulses.[8] Experimentally the system was checked out on an EAI581 analog computer with hysteresis realized using comparator controlled function relays. As such the results of Ref. 8 are impractical for microelectronic systems and hence are best considered as an "existence proof" for the validity of the ideas.

In the next section we review the basic ideas and equations from which the basic module is presented and further design equations given. Section III gives experimental results, with closing discussion in Section IV.

II. The Hysteretic Neural-Type Module

We begin with the basic first order state-variable like equations[8] written in a form most useful for our circuit

$$k\dot{x} = -\alpha x - \beta H(x) - \gamma u \tag{1a}$$

$$y = x \tag{1b}$$

here u = input, y = output, x = internal (state-like) variable, α,β,γ,k are nonnegative constants and $H(\cdot)$ is the multivalued binary hysteresis function

$$H(x) = \begin{cases} H_+ & x > x_+ \\ \{H_+, -H_-\} & -x_- < x < x_+ \\ -H_- & -x_- > x \end{cases} \tag{2}$$

(where $\{H_+,-H_-\}$ is the two element set comprised of H_+ and H_-). Figure 1 graphically presents $H(\cdot)$ the picture of which is important to our development.

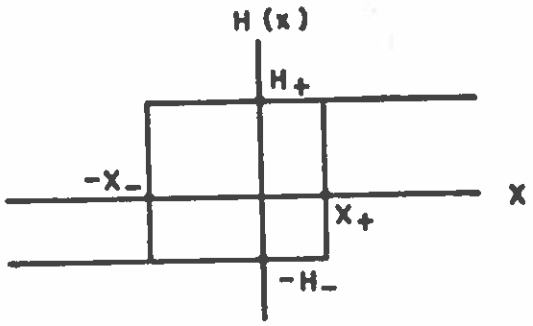

Fig. 1. Binary Hysteresis $H(\cdot)$.

Figure 2 gives for (1) a signal-flow graph representation in which we have included a nonlinear transmittance $H(\cdot)$.

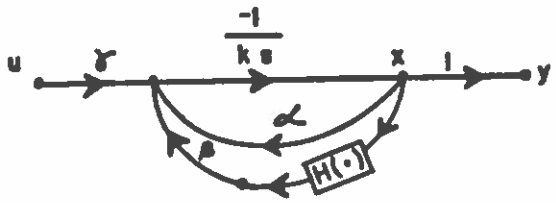

Fig. 2. Signal-Flow Graph for Equations (1).

All portions of this signal-flow graph except that for $H(\cdot)$ can be realized by an op-amp integrator with a summation input, as shown in Fig. 3a) where we have (using $G_i = 1/R_i, i = x,H,u$)

$$k = C,\ \alpha = G_x,\ \beta = G_H,\ \gamma = G_u \tag{3}$$

Figure 3 shows an op-amp means of realizing suitable hysteresis functions $H(\cdot)$.[9] To determine further the characterization of $H(\cdot)$ we consider the op-amp characteristic as that given by the set function

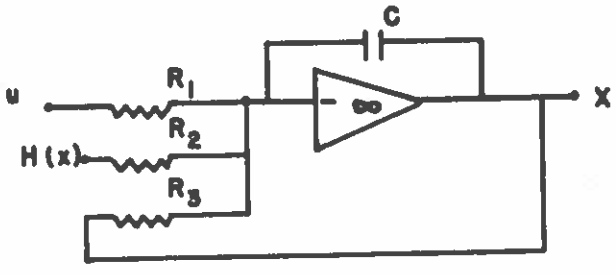

a)

CH1749-1/82/0000-0502 $00.75 © 1982 IEEE

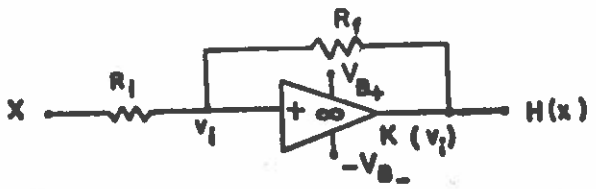

b)

Fig. 3. Flow-Graph Component Realizations.
a) Realization of Eq. (1a)
b) Realization of H(x)

$$K(v_i) = \alpha \begin{cases} V_+ , & 0<v_i \\ [-V_-,V_+], & 0 = v_i \\ -V_- , & v_i<0 \end{cases} \qquad (4)$$

where $[-V_-,V_+]$ is the interval of numbers between $-V_-$ and V_+; V_+ = positive saturation voltage, $-V_-$ = negative saturation voltage. According to Fig. 3, the op-amp characteristic is subject to the load line

$$K(v_i) = -\left(\frac{R_f}{R_i}\right) x + \left(1 + \frac{R_f}{R_i}\right) v_i \qquad (5)$$

Drawing this load line on the op-amp curve, as in Fig. 4, shows that the x-intercepts of $H(\cdot)$, x_- and x_+, are determined by the lines going through b-c and g-h respectively.

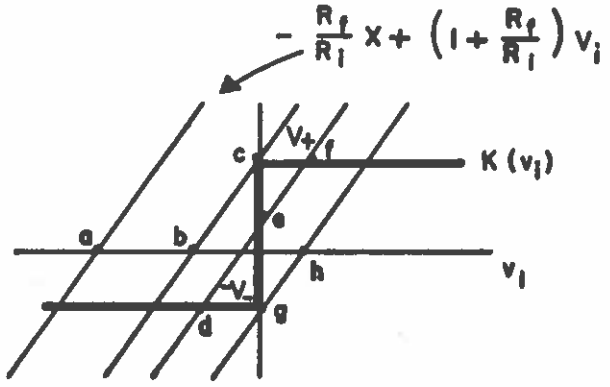

Fig. 4. Schema for Determination of Parameters for $H(\cdot)$

Using

$$K(0_+) = V_+ = H_+, \; K(0_-) = -V_- = -H_- \qquad (6a)$$

in (5) gives

$$x_- = \left(\frac{R_i}{R_f}\right) H_+ , \; x_+ = \left(\frac{R_i}{R_f}\right) H_- \qquad (6b)$$

The four parameters in $H(\cdot)$ of (2) are consequently fixed by the op-amp saturation voltages and the resistances of Fig. 3b). It should be noted that the line d-e-f of Fig. 4 shows that the two member set value of $H(\cdot)$ is really a three member set value--we ignore the third value as it is dynamically of little importance to our theory.

Returning to (1) we next investigate equilibrium points, these being the values of x for which $\dot{x} \equiv 0$. For this let us note (1) when $\dot{x}=0$ and define the load line L(x,u) by

$$L(x,u) = -\frac{\alpha}{\beta} x - \frac{\gamma}{\beta} u \qquad (7a)$$

Then if the input assumes a constant resting value u_R and x_E is the corresponding equilibrium state

$$H(x_E) = L(x_E,u_R) \qquad (7b)$$

is the equation determining x_E, as illustrated in Fig. 5.

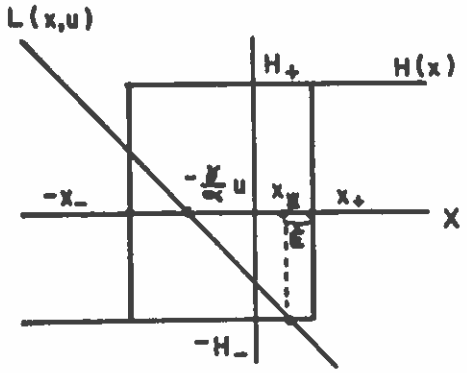

Fig. 5. Resting Point Determination.

Now, in order to cascade basic modules and have them all operating at the same equilibrium point we will choose

$$u_R = x_E \qquad (8a)$$

The geometry of Fig. 5 gives $-H_- = [-\frac{\alpha}{\beta} x_E - \frac{\gamma}{\beta} u_R]$ which with (8a) gives

$$u_R = x_E = \frac{\beta}{\alpha+\gamma} H_- = \frac{G_H}{G_x+G_u} H_- \qquad (8b)$$

Considering Fig. 5 further we see that there are a number of possible behaviors for a given input depending upon how the load line [of (7) in the resting state] intersects the hysteresis curve. The most interesting case is when there is one intersection of the type shown in Fig. 5; we might call this a triggered neural pulse generator.

Triggered Neural Pulse Generator

We require that the load line $L(x,u_R)$ of Fig. 5 intersects the lower, $-H_-$ portion of the hysteresis curve but not the upper, H_+ portion. Thus

$$L(-x_-,u_R) < H_+ \text{ and } L(x_+,u_R) < -H_- \qquad (9)$$

We also desire x_E slightly smaller than x_+. Setting

$$\varepsilon = x_+ - x_E > 0 \quad \text{(small)} \qquad (10)$$

and using (6), (8b), (3), we have

$$\frac{G_x}{G_H}\cdot\frac{G_f}{G_i}H_+ - \frac{G_u}{G_H}\cdot\frac{G_H}{G_x+G_u}H_- < H_+$$

and

$$-\frac{G_x}{G_H}\cdot\frac{G_f}{G_i}H_- - \frac{G_u}{G_H}\cdot\frac{G_H}{G_x+G_u}H_- < -H_- \qquad (11a)$$

$$\varepsilon = \frac{G_f}{G_i}H_- - \frac{G_H}{G_x+G_u}H_- > 0 \quad \text{(small)} \qquad (11b)$$

Assuming H_+ and H_- positive, these are rewritten as

$$0 < \frac{G_u}{G_x+G_u}\frac{H_-}{H_+} - \frac{G_xG_f-G_HG_i}{G_HG_i} \text{ and } 0 < \frac{G_u}{G_x+G_u} + \frac{G_xG_f-G_HG_i}{G_HG_i}$$

Rewritten again more conveniently this is, followed by (11b),

$$\left[1 - \frac{1}{1+(G_x/G_u)}\right]\cdot\frac{G_i}{G_f} < \frac{G_x}{G_H} < \left[1 + \frac{1}{1+(G_x/G_u)}\frac{H_-}{H_+}\right]\frac{G_i}{G_f} \qquad (12a)$$

$$0 < \frac{\varepsilon}{H_-} = \frac{G_f}{G_i} - \frac{G_H}{G_x+G_u} \qquad (12b)$$

Under these conditions an input change, Δu, needed to trigger an action potential like pulse is one that moves the load line $L(x,u_R+\Delta u)$ so that it no longer intersects the lower branch of the hysteresis curve, that is

$$\frac{-\gamma}{\alpha}\cdot\Delta u \geq \varepsilon = x_+ - x_F \qquad (13a)$$

or

$$\Delta u \leq -\frac{G_x}{G_u}\varepsilon = -\frac{G_x}{G_u}\left[\frac{G_i}{G_f} - \frac{G_H}{G_x+G_u}\right]H_- \qquad (13b)$$

In this case a negative going trigger pulse, of magnitude $G_x\varepsilon/G_u$ will trigger the load line to jump from the lower portion of the hysteresis curve to the upper. If the trigger input is short the system will return to equilibrium via a traversal of the hysteresis loop (under control of the dynamics of the capacitor) giving an action potential like pulse as the resulting output. The "height" of the output pulse is about that of the hysteresis width

$$W_H = x_+ + x_- = \frac{G_f}{G_i}(H_+ + H_-) \qquad (14)$$

III. Experimental Results

Figure 6 shows the circuit upon which measurements were made using an MC 1458 CP dual operational amplifier package for the two op-amps (with pin numbering as shown in the figure). When fed with pulses a Tektronix PG 508 Pulse Generator was used as the signal source while when fed by sine waves (as for the recording of the hysteresis loop) a Tektronix FG 502 Function Generator was used. All oscilloscope displays presented were recorded on a Tektronix 561A oscilloscope (with a faulty retrace which shows up on the photographs).

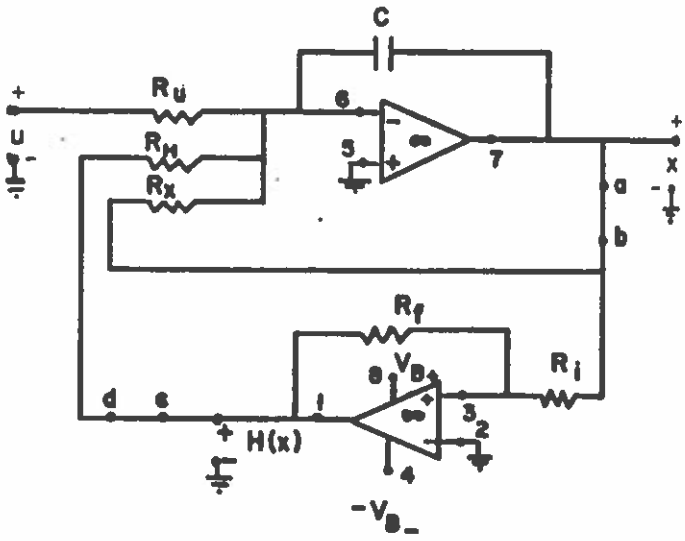

Fig. 6. Op-Amp RC, Hysteresis, Neural-Type Circuit.

The values $R_x = R_f = 20K\Omega$, resulting in $R_H=2R_u=2R=20K\Omega$, were used, along with two choices of C, 300 pf and 0.01 μfd. Figure 7a) shows the hysteresis loop, measured by inserting a 10Hz sine wave as input at point b of Fig. 6, with lead a-b open, and measuring the output at point c (with lead c-d connected). In order to hold to the design values of $H_+ = H_- = 4v$, as obtained in Fig. 7a), it was necessary to apply op-amp biases $V_{B+} = 4.6$ v and $V_{B-} = 6.0$ v; we will later discuss the case $V_{B+} = V_{B-} = 4$ v.

Figure 7b) shows a typical pulse response. Here the measured dc value of the input needed to obtain the same dc value of output was $u_R = x_E = 1.3$ which agrees very well with the value of 4/3 calculated in the design. The threshold level of the input change needed to trigger the output was somewhat under 0.4 v, in reasonable agreement with the calculated value of $|\Delta u|_{min} = 1/3$ previously found. The output pulse rise with an input at triggering threshold was found to be about 0.7 v, again in agreement with the calculated $\varepsilon = x_+ - u_R$; the rise in Fig. 7b) is larger than ε since the input trigger is larger than threshold. The minimum pulse width needed to trigger an output, for a one volt Δu, was measured to be 3μ sec. when C = 300 pf (and 0.07m sec. when C = 0.01 μf). Figure 7c) clearly shows that a steady input above threshold magnitude gives rise to a repetitive output.

Changing to C = 0.01 μf Fig. 8 shows the obtained pulses in more detail. Figure 8a) shows a pulse obtained for an input of magnitude just at the trigger level. Figure 8b) shows the detail of a sequence of pulses obtained by a trigger of the same pulse width as in part a) but of greater magnitude. With a very much greater input magnitude a signle output pulse results which is of width equal to the input pulse width. In Fig. 8c) the effect of a high input pulse repetition rate is shown, the circuit exhibiting a refractory period.

It should be noted that in Fig. 6 the integrating op-amp and the hysteresis op-amp use the same dual

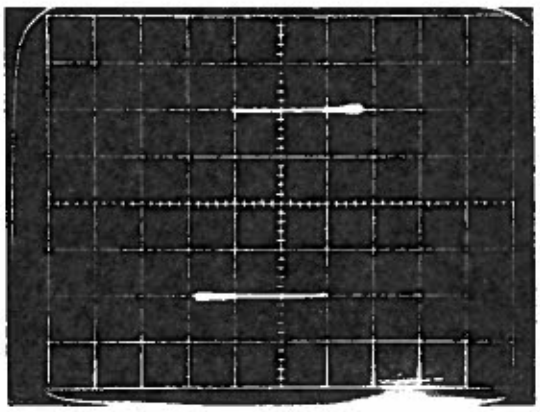

a)

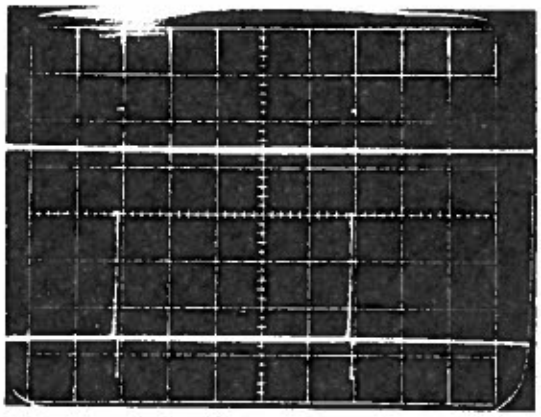

b)

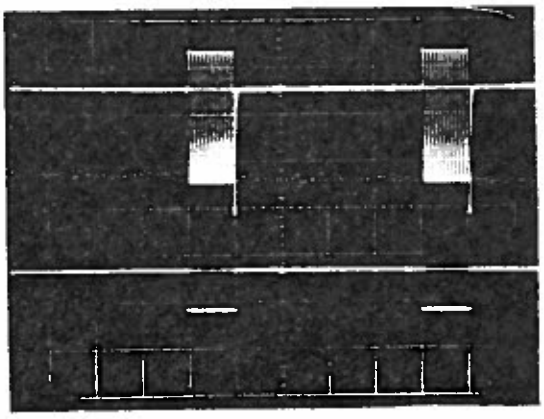

c)

Fig. 7. Measured Circuit Characteristics:
$R_x=R_f=R_{B_-}=2R_u=2R_i=20K\Omega$
Scales: 2v/div or 0.5 m sec/div
a) In Place Hysteresis ($V_{B_+}=4.6$, $V_{B_-}=6.0$)
(Horizontal = x, Vertical = H(x);
(0,0) at center)
b),c) Typical responses, C = 300 pf
Lower trace = u, 0 on second line up
Upper trace = x, 0 on second line down

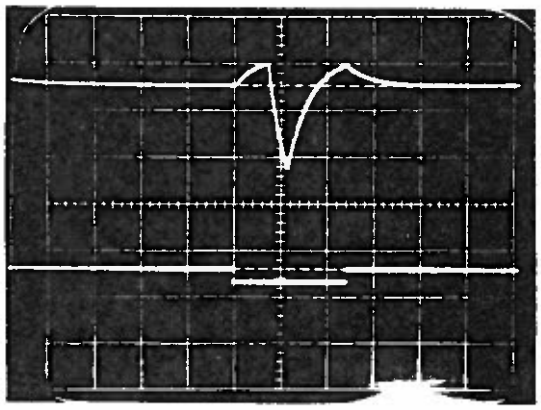

a)

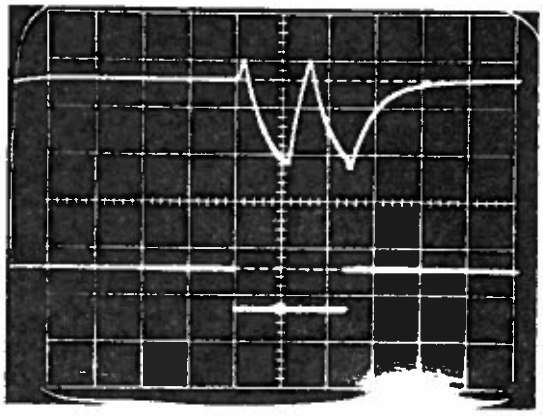

b)

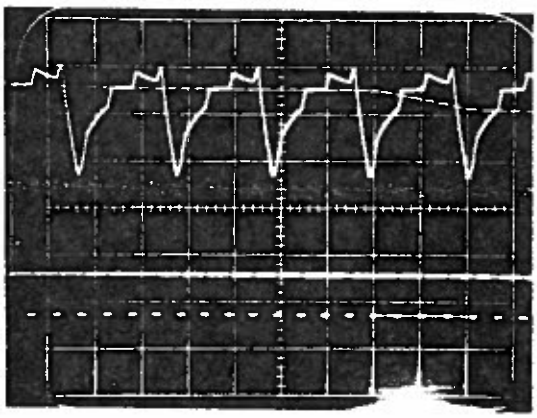

c)

Fig. 8. Further Measured Characteristics, C = 0.01
Scales: As in Fig. 7
a) At Threshold Magnitude
b) Above Threshold
c) Refractoriness

power supply (an HP6237B being used). This is possi
even though the hysteresis amplifier must saturate
while the integrating amplifier remains in linear
operation since the hysteresis width is chosen suffi-
ciently narrow, that is a four volt peak-peak signal
saturates the hysteresis amplifier while about a ten

volt peak-peak signal is needed to saturate the integrating amplifier.

The structure works equally well when the resistance values are scaled up by a factor of ten. When scaled down by a factor of ten it also operates satisfactorily, except that loading effects make the design equations not as accurate. If necessary, the accuracy can be restored by the insertion of another op-amp pair of unity-gain isolation amplifiers, one replacing the line a-b and one c-d in Fig. 6. In the absence of these isolation amplifiers we have noticed that there is more control on the pulse repetition rate versus input amplitude for the lower resistance valued circuit.

For the op-amps used the output saturation levels were not equal to the supply values. Consequently, $H_-\neq V_{B_-}$, $H_+\neq V_{B_+}$. Figure 9 shows that this effect cannot be ignored since $V_{B_-}=V_{B_+}=4v$ gives $H_-=3.3v$ and $H_+=2.1v$. Nevertheless only slight modifications in element values are needed to make the circuit perform satisfactorily with $V_{B_-}=V_{B_+}$. Since the design equations are in terms of H_- and H_+, once the true hysteresis curve is known design can proceed from the equations of section II.

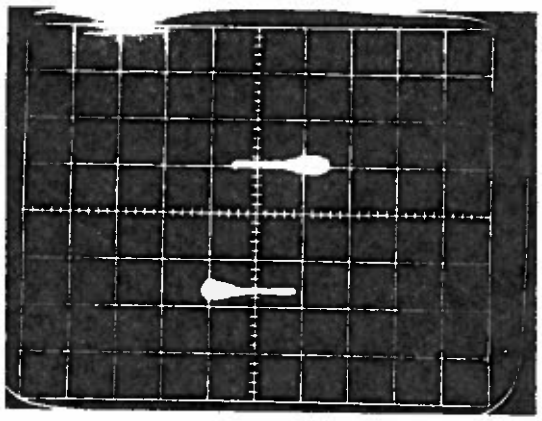

Fig. 9. In Place Hysteresis, as in Fig. 7 but $V_{B_-}=V_{B_+}=4$.

IV. Discussion

In Section II we have presented a design procedure leading to working op-amp RC neural-type circuits. This design is based upon the use of hysteresis which is biased to a stable resting state for triggered pulse response.

In triggered responses the circuit exhibits many of the customary neuristor type of responses as well as having a repetitive response over a range of input pulse magnitudes. Although this type of response has been reported previously[6,7,10,11], the circuit studied here appears to be the most controllable.

The circuit studied here has shown us a high degree of robustness in that reasonable variations in parameters have still allowed it to work essentially as designed. Consequently, we believe the use of hysteresis, which has allowed a simple first order circuit to result, seems to hold considerable promise for the field of neural-type microsystems.

V. References

1. R. W. Newcomb, "Neural-Type Microsystems: Some Circuits and Considerations," Proceedings of the 1980 IEEE Conference on Circuits and Computers, New York, October 1980.

2. R. W. Newcomb, "MOS Neuristor Lines" in "Constructive Approaches to Mathematical Models C. V. Coffman and G. J. Fix, editors, Academic Press, 1979, pp. 87-111.

3. C. Czarnul, G. Kiruthi, and R. Newcomb, "MOS Neural Pulse Modulator," Electronics Letters, Vol. 15, No. 25, December 6, 1979, pp. 823-82-.

4. N. DeClaris, "Neural-Type Junctions - A New Circuit Concept," Proceedings of the Midwestern Symposium on Circuits and Systems, August 1976.

5. N. Dimopoulos and R. W. Newcomb, "Stability Properties of a Class of Large Scale Neural Networks," Proceedings of the IEEE International Symposium on Circuits and Systems, Houston, April, 1980, pp. 526-530.

6. C. K. Kohli, "An Integrable MOS Neuristor Line: Design, Theory and Extensions," Ph.D. Dissertation, University of Maryland, 197-.

7. G. Kiruthi, H. Yazdani and R. W. Newcomb, "A Hysteresis Circuit Seen Through Semi-State Equations," Proceedings of the 23rd Midwest Symposium on Circuits and Systems, Toledo, August 1980, to appear.

8. C. K. Kohli, R. C. Ajmera, G. Kiruthi and R. W. Newcomb, "Hysteretic System for Neural-Type Circuits," Proceedings of the IEEE, Vol. 69, No. 2, 1981, pp. 285-287.

9. T. Kohonen, "Digital Circuits and Devices," Prentice-Hall, Englewood Cliffs (N.J.), 197-.

10. C. K. Kohli and R. Newcomb, "Voltage Controlled Oscillations in the MOS Neural Line," Proceedings of the IEEE Midwestern Symposium on Circuits and Systems, 1977, pp. 134-136.

11. Z. Czarnul and M. Bialko, "Utilization of a Single Inductorless Neuristor Line Section as a Voltage to - Frequency Converter," Electronics Letters, Vol. 13, 1977, pp. 251-252.

CONFERENCE PROCEEDINGS
IEEE SOUTHEASTCON '82

April 4-7, 1982
Sandestin
Destin, Florida

The Institute of Electrical and
Electronic Engineers, Inc.
82CH1749-1